Design a Grid Tie Inverter for PMSG Wind Turbine using FPGA & DSP Builder

Ilhami Colak
Faculty of Engineering, Department of Electrical & Electronics Engineering
Istanbul Gelisim University, Istanbul-Turkey
icolak@gelisim.edu.tr

Eklas Hossain
PhD Candidate
Center for Sustainable Electrical Energy Systems,
University of Wisconsin Milwaukee, USA
shossain@uwm.edu

Ramazan Bayindir
Faculty of Technology, Department of Electrical & Electronics Engineering
Gazi University Ankara-Turkey
bayindir@gazi.edu.tr

Jakir Hossain
BSc in EEE
Khulna University of Engineering and Technology, Khulna-9203, Bangladesh
engrhossainjakir@gmail.com

Abstract – **The recent makeshift in fuel choice, renewable energy sources has been considered as the most popular form of its kind because of its environment friendly approaches, less cost tariff policy and the natural fuel abundance. This inclusion in power system promotes Micro-grid system to optimize the overall distribution. FPGA, elaborated as Field Programmable Gate Array, proposes chances for enhanced performance and coveted flexibility in design for the digital control. Conversely, the erudite convolution of the Hardware Description Language (HDL) coding, a way translating to HDL, can be an undesirable hurdle for the professional system designers. The design, depicted in this letter, is an instance of system modeling for FPGA-based digital control, which necessarily has the desired ability to auto-generate the HDL codes. The architecture of this design uses the DSP Builder technology, in a MATLAB / SIMULINK platform. A three phase full-bridge gird tied inverter for wind system and a three phase full-bridge inverter for grid connected wind system are built that demonstrates the close correlation with the model. The necessary simulations, results and the experimental analysis have also been highlighted for the different control techniques such as PI, dq, and the PWM control technique.**

***Index Terms*– Renewable Energy, Microgrid, PI Control, dq Control, PWM control Technique, FPGAs in Industrial Control Systems, Controller Hardware/Software, ALTERA DSP BUILDER.**

I. INTRODUCTION

As the fossil fuel cost increases, the oil insecurity intensifies, and the continually increasing concerns about the climate change cast a dark shadow over the future of available coal, with a sagacious makeshift in fuel choice, now, a new energy economy is emerging. At present, the old energy economy fueled by the oil, the coal, and the natural gas is gradually being replaced by one powered by the renewable natural resources, such as the wind and the solar [1].

On the other hand, FPGA, a free and unaffiliated ocean of gates, is programmed combining the gates all together to assemble the tools such multipliers, adders, registers, etc. [3]. On this occasion, this assembly can readily be done exploiting HDL, elaborated as Hardware Development Language, which allows for parallel operation and surely places a significant resource for the operation. Despite that, the intricacy of HDL, in purpose of coding and compilation, can be a hurdle for the engineers and the system designers. To get rid of that complexity, tools for rapid prototyping FPGA, in purpose of control and flexible in variable speed conditions, have been promoted [4] and the usage of FPGA has commenced to invade necessary control of the power electronics and the miscellaneous featured functions [5]. Fig. 1 represents a comparison between fossil fuel and renewable energy.

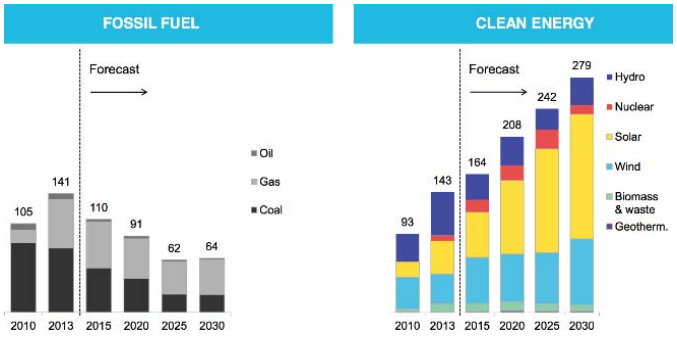

Fig. 1. Fossil fuel vs Renewable energy

Total surface area of the earth is 5.1E14 m2 [proper format] where the land surface area is 1.49E14 m2 only. The minimum solar radiation is 1321 w/m2. In particular, the Earth draws 174 petawatts (PW) of incoming solar radiation (insolation) at upper atmosphere. But, roughly 30% of that is reflected back to space and the rest 70% is absorbed by the oceans, the clouds, and the land masses. Besides that, the solar light spectrum at the Earth's surface is spread across the visible and near-infrared ranges with a limited portion in the near-ultraviolet boundary. Therefore, about half the incoming solar energy reaches the Earth's surface indicates 89 petawatts [1, 2]. By statistics of 2013, the installed photovoltaic capacity was 139 gigawatts on the planet. For 2014, another estimated 35 to 52 GW would to be installed. Hence, at 2014, the total photovoltaic capacity culminated at 174 gigawatts [3]. So, in a nutshell, the total available solar pick power in this earth= 89 Petawatts (PW) and the total harvested capacity of photovoltaic power = 174 gigawatts (GW)

From this current picture, the percentage of the harvested solar

978-1-5090-1798-0/16/$31.00 ©2016 IEEE

$$\text{power} = \frac{\text{Total harvested photovoltaic power}}{\text{Total available solar power in this earth}}\ 100\%$$

$= \frac{174\ \text{GW}}{89\ \text{PW}} * 100\%$ = 0.00019%. Where, the total pick power consumption by the entire civilization = 15 terawatts (TW). So, The estimated percentage of the exploiting solar power

$$= \frac{\text{Amount of solar power currently in used}}{\text{Amount of power currently used by entire civilization}}\ 100\%$$

$$= \frac{174\ \text{GW}}{15\ \text{TW}} * 100\% = 1.16\%$$

Solar energy has ability to provide the total consumption power for the society alone and besides as the cost of solar energy falls sharply, the progress rate of harvesting solar energy has increased a lot. Inasmuch, the researchers have dubbed this point the saturation wind power potential. The saturation potential is more than 250 terawatts according to their statement, if we could install an army of 100-meter-tall wind turbines across the whole land and the water of planet Earth. Preferably, if we placed them only on land (minus Antarctica) and along the entire coastal ocean, there is still some 80 terawatts (TW) accessible [4]. By the year 2013, worldwide nameplate capacity of the wind-powered generators was 318 gigawatts (GW) that meant, growing by 35 GW over the preceding year [5].

By statistics, Percentage of the harvested wind power

$= \frac{\text{Total harvested wind power}}{\text{Total available wind power in this earth}}\ 100\% = \frac{353\ \text{GW}}{250\ \text{TW}} * 100\% =$ 0.14%, and on this occasion, by the same token of mathematical equation, the estimated percentage of the exploiting wind power

$= \frac{\text{Amount of wind power currently in used}}{\text{Amount of power currently used by entire civilization}}\ 100\%$

$= \frac{353\ \text{GW}}{15\ \text{TW}} * 100\% = 2.35\%$.

Wind energy has ability to provide the total consumption power for the space single-handedly and in addition as the cost of wind energy falls slowly, the progress rate of harvesting wind energy has increased reasonably. Typical wind farm will produce 2 w/m2 power and solar photovoltaic farm around 5 w/m2 power on average [6].

Altera's Digital Signal Processing Builder Technology implements the graphical depiction blocks plus the capacity to precisely auto-generate the regarding HDL code in MATLAB or SIMULINK platform. The DSP Builder, literally, has a very profound library of necessary general control operations to accelerate the entire development of the required control applications. Extensive application of the DSP Builder can implement a comprehensive system configuration that ensures the discernment of the model prior to the required hardware. Here, in this letter, it illustrates a relatively advanced methodology to develop an FPGA-based control with the application the Altera's exclusive DSP Builder. The necessary illustration of this DSP Builder and the block-set are depicted here. Inasmuch, a single-phase gird tied inverter for solar system and a three phase full-bridge inverter for grid connected wind system were assembled and the precise correlation to the presented model was manifested.

II. SYSTEM MODELING

A. WIND TURBINE MODEL:

A wind turbine (WT), is an electromechanical system and it generates the electric power owing to kinetic energy of the wind. In this case, the air density of wind crossing through the blades gets the rotor to move and magnetizes the stator windings that generate the output power [11]. The output power of a wind turbine can be calculated by using Equation (1). The mechanical power extracted from wind "Pω", which is a function of both the wind and the rotor speeds, can be approximated as follows:

$$P_\omega = 0.5\ \rho A_r C_p(\alpha, \beta) v^3 \quad (1)$$

$$\lambda = \frac{\omega_m}{v} R \quad (2)$$

$$C_p = C_1 \left(\frac{C_2}{\gamma} - C_3\beta - C_4\right) e^{\frac{C_5}{\gamma}} + C_6\lambda \quad (3)$$

Where,

ρ= Air density (kg/m3),
A= Rotor swept area (m2),
Pm= mechanical output power of wind turbine,
λ= Tip speed ratio,
Cp= Coefficient of performance (the rotor efficiency),
β= Pitch angle

The wind turbine mechanical torque output Tm is given as:

$$T_m = \frac{P_\omega}{\omega_m} = \frac{0.5\rho A_r C_p(\alpha,\beta).v^3}{\omega_m} \quad (4)$$

B. MICROGRID IN UWM

The Fig. 2 illustrates the various conditions. Fig.2(a) shows the variation of maximum power with change in rotor diameter. It shows impressive power for larger rotor diameter. Similarly, Fig 2(b) depicts the relation between hub height, wind speed, and generated power. Fig. 2(c) and Figure 2(d) shows the estimated annual energy production and wind power curve, respectively.

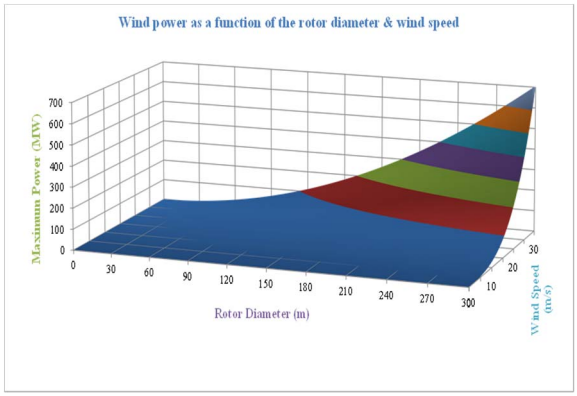

(a)

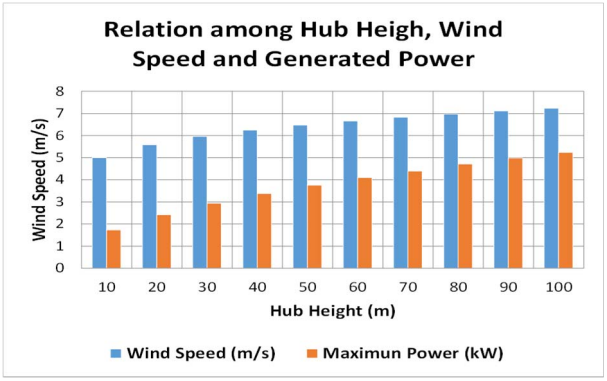

(b)

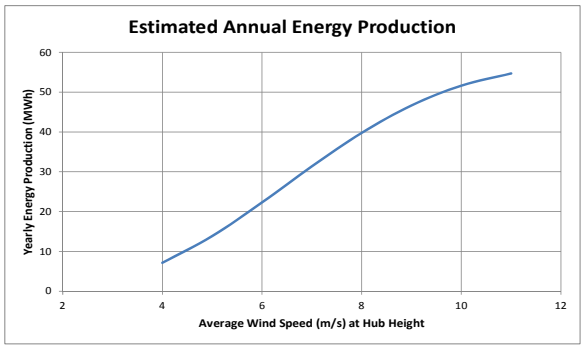

(c)

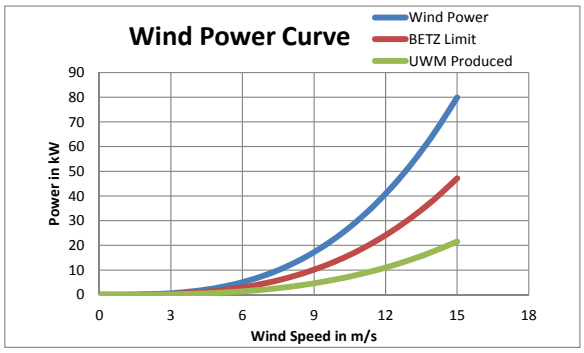

(d)

Fig. 2. Relation among rotor diameter; wind speed and generated power, Relation among hub height, wind speed and generated power; Estimated annual wind energy and Wind power curves at University of Wisconsin Milwaukee(UWM) have shown

C. PMSG MODELING

The electrical power equation for A HAWT is obtained

$$P_{out} = \frac{1}{2}\rho\pi r^2 v^3 C_p \qquad (11)$$

The radius is derived to be

$$r = \sqrt{\frac{2P_{out}}{\rho\pi v^3 C_p}} \qquad (12)$$

Considering 11 m/s as the rated speed, a 10 kW wind turbine has a blade radius of

$$= \sqrt{\frac{2x10000}{1.225x3.1416x11^3x0.288}} \approx 3.5m \qquad (13)$$

The Schematic diagram of PMSG WT has given below in Fig. 3. Wind comes to the wind turbine and there is a pitch control. From there, the generator and grid side part do their respective function.

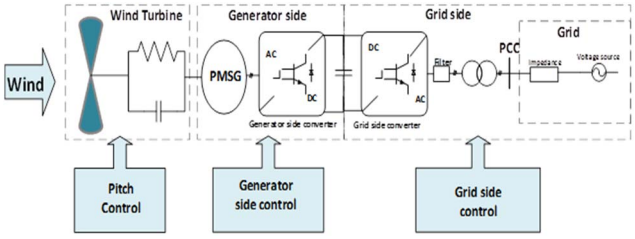

Fig. 3. Schematic diagram of PMSG

D. INVERTER AND CONTROL TOPOLOGY

Fig. 4, below, depicts an elementary design of the coveted inverter topology, so as the model of current controller. This simplified design is comprised of the floating direct current source, sequentially appearing from a particular solar (cell) array, besides that, a topology, H-bridged, linked to the specific grid accompanying the inductors. Here, the considering grid voltage is, one by one, sampled, at first, and then handled with PLL to generate a sinusoidal waveform for the necessary command reference. So, in this arrangement, the inverter current is to be sampled, and then treated with an LPF and correlated to command including error-amplifying device. Here, the relative miscue is employed to a sequentially connected PI regulator to construct a signal (V-Control) for the Pulse Width Modulator.

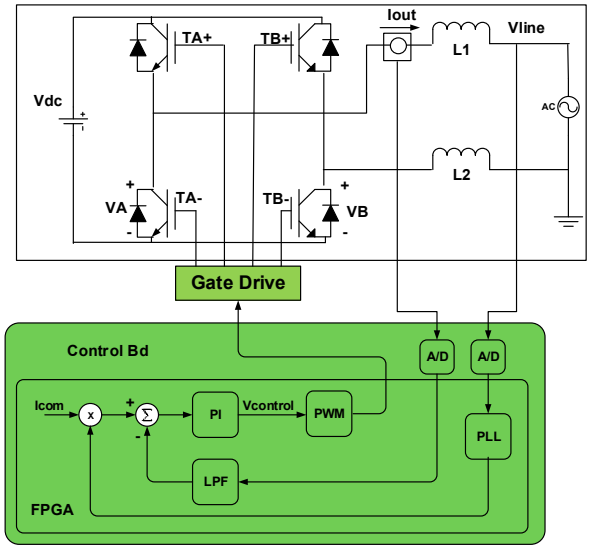

Fig. 4. Simplified Full-Bridge PWM Inverter

E. CONTROL SYSTEM REVIEW (FB PWM AMPIFIER)

The inverter with the full-bridge Pulse Width Modulation switching, the two legs (presuming A & B) of the full-bridge are measured distinctly using reflected control voltage (vcontrol), which is correlated to the triangle wave (VI") [6]. In this comparison, the output voltage of leg A is described by the equation (1), and the result is shown in Fig. 5b.

vcontrol > vtri: TA+ on and VAN = V_{dc}

vcontrol < vtri: TA- on and VAN = 0

In like manner, the Equation (2) delineates the output voltage of leg B, also shown in Fig. 5c.

-vcontrol > vtri: TB+ on and VBN = V_{dc}

- vcontrol < vtri: TB- on and VBN = 0

Fig. 5d illustrates the inverter PWM output, which is tied to the line through inductors L 1 and L2. The simpler Full-Bridge PWM Inverter is shown in Fig. 7.

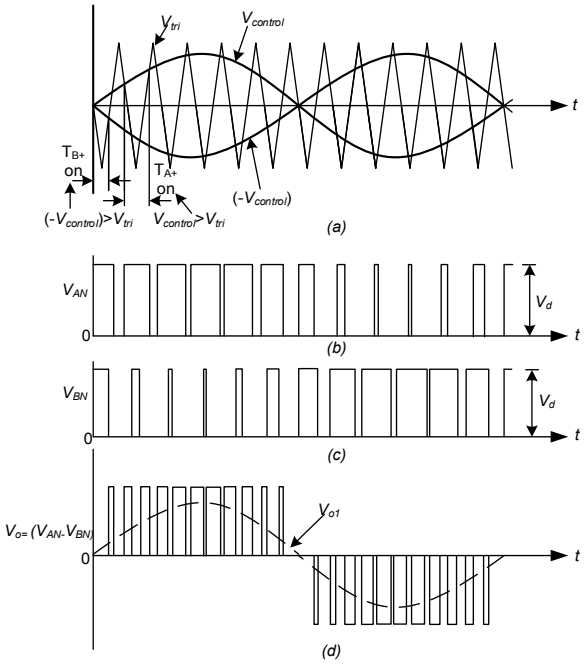

Fig. 5. Full Bridge PWM Switching Waveforms

F. DESIGN IMPLEMENTATION METODOLOGY

In this letter, the design, presented for the control purpose, was carried out using Altera's comprehensive DSP Builder toolbox in the virtual platform. Here, the subsystem, dedicated in purpose of control, from the model, delineated in section II, was distinctly replaced by the graphical blocks, available in the DSP Builder toolbox. Necessarily, it includes a Low Pass filters, PI controller, and the PWM generator. Figs. 3 and 4 illustrates the model comingled the PI controller and the PWM generator employed with the available DSP builder blocks.

III. ALTERA DSP BUILDER

This Digital Signal Processing Builder tool is retrieved from Mathworks Simulink and it permits the designer to improve, confirm and assimilate the model into hardware, while the remaining in the Simulink platform. It also indicates the design of the circuits, dedicated for the purpose of control, which can be combined with other designs, fashioned in SIMULINK platform, of the power electronics and any machine-driven components of the entire system. DSP Builder inherently avoids compiling the insignificant details, in particular the lower level cases, of FPGA framework, hence the design engineers can solely focus on their algorithm buildup process. By this way, this extensive tool assures the superior performance and doesn't require expertise on the conventional HDL or FPGA. In this process, the output, necessarily a VHDL file, can be straightly amassed by Quartus II and implemented to program the FPGA. The basic function and environment of DSP Digital Control Design environment is illustrated in Fig. 6. Total environment describes in a very simple form using different block diagram.

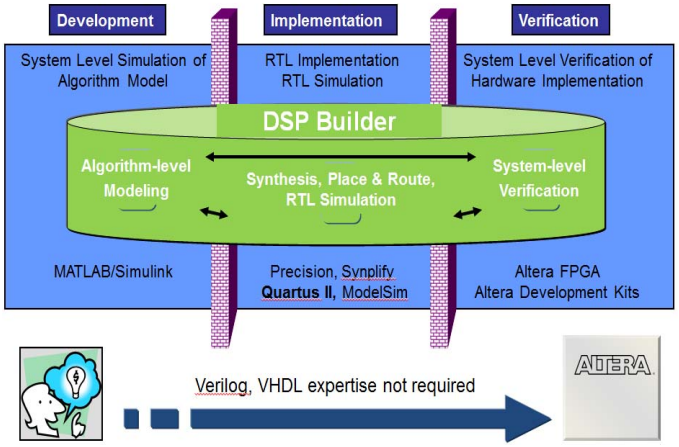

Fig. 6. Integrated development environment within Simulink

After that, the three phase current is presented in Fig. 7(a). Here, both of the real and reactive power control is presented in the block. On this occasion, grid converts the photovoltaic and wind power system. Next, in sequence, Fig. 7(b) illustrates the Simulink block diagram for particular case of three phase current control. Each block in that illustration represents the individual function of the total system.

IV. PROTOTYPING AND TESTING

The Results, illustrated in the previous section, from the inverter experimentation are depicted in Fig. 8 below. Here, the regarding signals resemble to the grid voltage (here, channel 2), (in this experiment) the inverter output voltage (channel 3), and (according to the figure) inverter output current (channel 4). On this occasion, the waveforms, resulted from the experiment, exhibit correlation to the following simulation of Fig. 8.

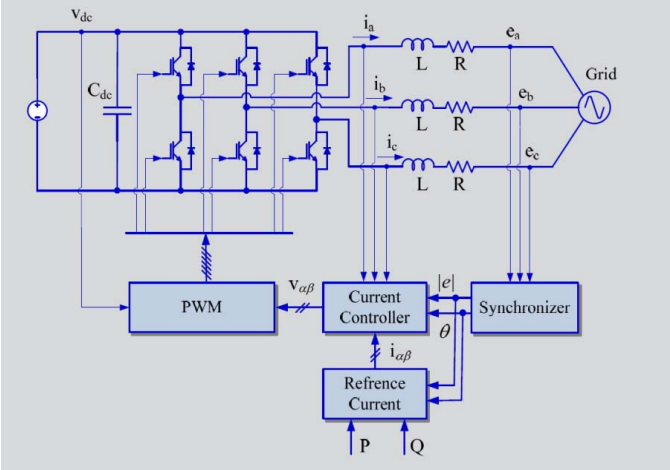

(a)

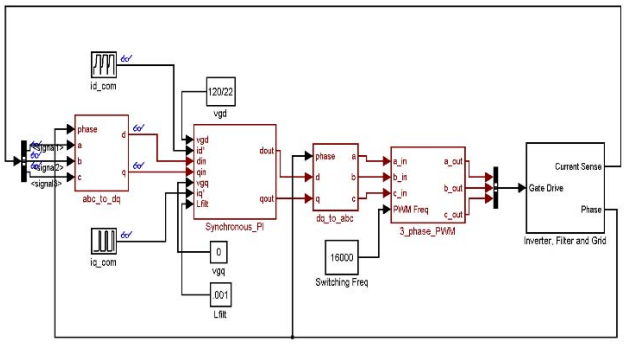

(b)

Fig 7. (a) Three phase current control. (b) Three phase current control using DSP

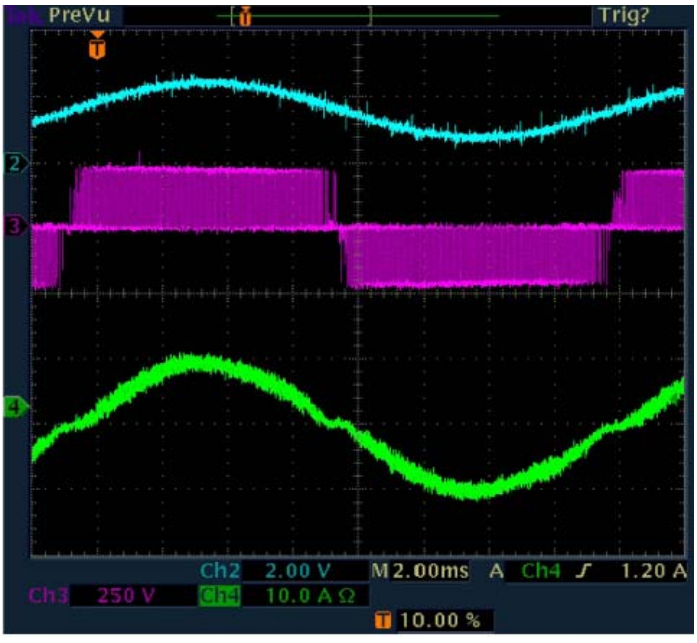

(a)

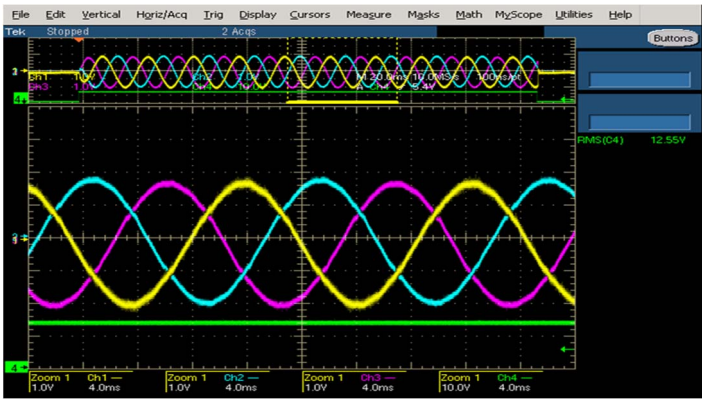

(b)

Fig. 8. Simulation result of 3-phase current controlled inverter

Fig. 9 for three phase current control circuit: Inverter Current in A, Power Output in kW, Comparator and Conversion of Idq to Iabc, Synchronous PI Control Output. Fig for booster circuit: boosting current in A, output voltage in V, comparator ratio.

TABLE 1
FULL-BRIDGE MODEL PARAMETER

Name	Value	Unit
DC Voltage	200	V
DC Capacitor	2400	uF
Output Inductance	400	uH
Line Voltage	120	Vrms
Line Inductance	5	uH
Carrier frequency	30	kHz
Line frequency	60	Hz

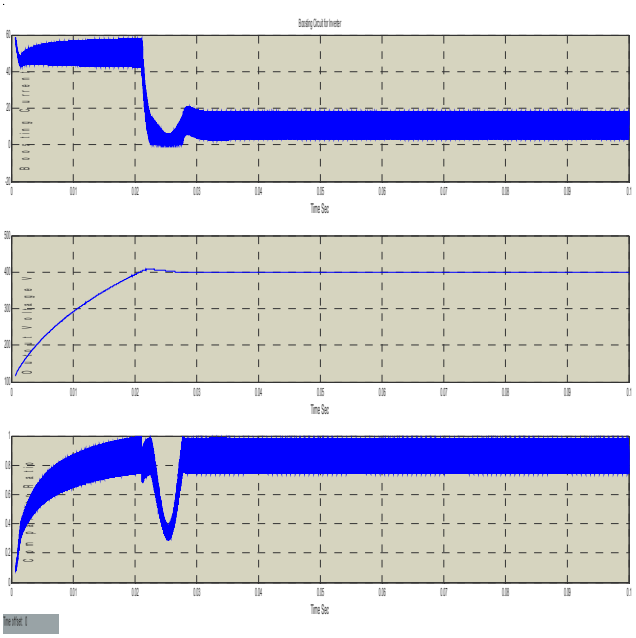

Fig. 9. Simulation result of 3-phase current controlled inverter

A simulation was made using the Simulink tool, so we could see and simulate the project before it was built, and also we could

analyze data and compare to see if we acquired something near to the reality. This is how the general part of the simulation looks: It is composed by a synchronous PI, a three phase PWM generator and inverter, filter and grid. The synchronous PI block takes all that is coming in and transforms to I_{dout} and I_{qout}. And it happens because of certain steps.

V. CONCLUSION

In this paper, the percentages of the harvested and the effectively exploited solar power have been reckoned. Besides that, the similar estimation has been shown for the wind energy. In this particular case, the blade radius of the wind turbine has been estimated from the derived equation to ensure the maximum efficiency. After that, the Modeling of PMSG WT has been completed for UWM. Here, an FPGA-based power electronics oriented controller has been successfully carried out on an Altera Stratix II FPGA. In this case, the operation of an FPGA for this function arranges hardwired parallel applications and the functional isolation of systematic multiple operations. Furthermore, an approach of establishing an HDL based controller for power electronics operations using the Altera's DSP Builder technology was manifested. The DSP Builder, a very powerful tool to adopt such kind of operation, ensures a harmonized simulation platform of HDL with MATLAB/SIMULINK. Besides that, it can also truncate the design cycle by assuring the auto-generation of the required HDL code. Here, three phase grid tie inverter for WT has been modeled and pragmatically enabled. The necessary simulations, results and the experimental analysis have also been depicted for the different control techniques such as PI, dq, and the PWM control technique [7 - 15].

REFERENCES

1. Mekonnen, Ezana T., Jason Katcha, and Michael Parker. "An FPGA-based digital control development method for power electronics", IECON 2012 - 38th Annual Conference on IEEE Industrial Electronics Society, 2012.
2. Kabalci, Ersan. "Design and analysis of a hybrid renewable energy plant with solar and wind power", Energy Conversion and Management, 2013.
3. OUCHI, Shigeto, Nariyuki KODANI, and Hiroshi HIRATA. "Anti-sway Control for a Rotational Crane Based on the Back-stepping Approach", Transactions of the Society of Instrument and Control Engineers, 2013.
4. Colak, Ilhami, and Ersan Kabalci. "Control Methods Applied in Renewable Energy Systems", Green Energy and Technology, 2014.
5. Eklas Hossain, Ersan Kabalci, Ramazan Bayindir and Ronald Perez "Microgrid testbeds around the world: State of art", Energy Conversion and Management 86 (2014) 132–153.
6. Eklas Hossain, Ersan Kabalci, Ramazan Bayindir and Ronald Perez "A Comprehensive Study on Microgrid Technology", International Journal of Renewable Energy Research, Vol.4, No.4, 2014 1094–1107.
7. Eklas Hossain, Sheroz Khan and Ahad Ali "Low voltage power line characterization as a data transfer method in public electricity distribution networks and indoor distribution networks", Electric Power Conference in Canada, 2008. (EPEC) 2008, Pg. No. 1-7.
8. Eklas Hossain, Sheroz Khan and Ahad Ali "Modeling Low Voltage Power Line as a Data Communication Channel", World Academy of Science, Engineering and Technology) 2008, Vol. 45, Pg. No. 148-152.
9. Eklas Hossain, Riza Muhida, Ahmad Faris Dzulkipli and Khairul Azizi Abdul Rahman "Solar cell efficiency improvement using compound parabolic concentrator and an implementation of sun tracking system", International Conference on Computer and Information Technology (ICCIT) 2008, Pg. No. 723-728.
10. Eklas Hossain, Riza Muhida, and Ahad Ali "Efficiency improvement of solar cell using compound parabolic concentrator and sun tracking system", Electric Power Conference in Canada, 2008. (EPEC) 2008, Pg. No. 1-8.
11. Ersan Kabalci, Ramazan Bayindir and Eklas Hossain "Hybrid microgrid testbed involving wind/solar/fuel cell plants: A desing and analysis testbed", International Conference on Energy Research and Application (ICRERA), 2014, Pg. No. 880-885.
12. Ersan Kabalci, Eklas Hossain and Ramazan Bayindir "Microgrid test-bed design with renewable energy sources", International Conference on Power Electronics and Motion Control Conference and Exposition (PEMC), 2014, Pg. No. 907-911.
13. Eklas Hossain, Ramazan Bayindir, Ersan Kabalci and Erdal Bekiroglu "Microgrid facility at European union", International Conference on Energy Research and Application (ICRERA), 2014, Pg. No. 873-879.
14. J. Hossain, S. S. Sikander and E. Hossain, "A wave-to-wire model of ocean wave energy conversion system using MATLAB/Simulink platform," *2016 4th International Conference on the Development in the in Renewable Energy Technology (ICDRET)*, Dhaka, Bangladesh, 2016, pp. 1-6. doi: 10.1109/ICDRET.2016.7421492
15. Ramazan Bayindir, Eklas Hossain, Ersan Kabalci, and Kazi Md Masum Billah "Investigation on North American Microgrid Facility", International Journal of Renewable Energy Research, Vol.5, No.2, 2015 558-574.